MultiResolution Complexity Analysis
A Novel Method for Partitioning Datasets into Regions of Different Classification Complexity

G. Armano and E. Tamponi
Department of Electrical and Electronic Engineering, University of Cagliari, Cagliari, Italy

Keywords: Data Analysis, Preprocessing, Complexity, Estimation.

Abstract: Systems for complexity estimation typically aim to quantify the overall complexity of a domain, with the goal of comparing the hardness of different datasets or to associate a classification task to an algorithm that is deemed best suited for it. In this work we describe *MultiResolution Complexity Analysis*, a novel method for partitioning a dataset into regions of different classification complexity, with the aim of highlighting sources of complexity or noise inside the dataset. Initial experiments have been carried out on relevant datasets, proving the effectiveness of the proposed method.

1 INTRODUCTION

Many experimental works on classification algorithms attempt to analyze the behavior of classifiers by studying their performances on different domains. However, the reasons behind the classifier's success (or failure) are rarely investigated. The connection between data characteristics and classifier design and performance has received attention only recently (Sohn, 1999). The aim of this emerging research area is to discover and analyze characteristics of the data that are related to its *classification complexity*.

A very simple measure of data complexity is the accuracy (or some other performance metric) of the adopted classifier on the dataset at hand. However, this measure does not give any insight on the reasons for which the classifier achieves that performance. Moreover, theoretical studies most often reach very loose bounds, that are not useful in practice (i.e., the Bayes error (Fukunaga, 1990); a notable work by Tumer (Tumer and Ghosh, 1996) aims at estimating the Bayes error through classifiers combination).

A work by Ho details how some measures can help discriminate an easy problem from difficult ones, for example, average number of points per dimension, maximum Fisher's discriminant ratio, non-linearity of nearest neighbor classifier (Ho and Basu, 2000). In another work, Ho shows how to use these metrics to select between different kinds of ensemble classifiers for a particular classification task (Ho, 2000).

In order to find complexity measures easier to calculate than the Bayes error, various authors compare their metrics to the Bayes error itself (which is considered the golden standard). Of course, this kind of comparison is only possible with domains for which the Bayes error can be calculated with analytical or numerical methods, or on datasets for which lower and upper bounds on the Bayes error are relatively close to one another (Bhattacharyya, 1943).

On the other hand, Singh (Singh, 2003) calculates a complexity metric by partitioning the feature spaces into hyper cuboid, and proves the effectiveness of his metric by showing its correlation with the performance of a real classifier on unseen test data.

In the recent years, various complexity measures have been applied to compare classifiers in order to find the optimal classification algorithm for a given domain (Mansilla and Ho, 2005), (Luengo and Herrera, 2012). In (Sotoca et al., 2006), the authors describe an automatic framework for the selection of an optimal classifier. Finally, in (Luengo et al., 2011) the authors apply the measures of complexity to analyze the behavior of various techniques for imbalance reduction.

In general, the current literature on the topic considers a dataset as a whole, to either find the most important characterization of its complexity, as in the case of (Ho and Basu, 2000), or to rank datasets by their "overall" complexity.

In fact, instead of estimating the overall complexity of a domain, we aim at estimating its local characteristics, in order to find high-complexity regions

Armano G. and Tamponi E..
MultiResolution Complexity Analysis - A Novel Method for Partitioning Datasets into Regions of Different Classification Complexity.
DOI: 10.5220/0005247003340341
In *Proceedings of the International Conference on Pattern Recognition Applications and Methods* (ICPRAM-2015), pages 334-341
ISBN: 978-989-758-076-5

inside a dataset. This can be viewed as a particular way of exploiting boundary information (Pierson et al., 1998), which has been used in other works to extrapolate a measure for the whole dataset (Pierson et al., 1998).

In this work we propose *MRCA* (i.e., MultiResolution Complexity Analysis), a method for identifying regions of different complexity in a dataset. The remainder of the paper is organized as follows: Section 2 illustrates the proposed method for identifying regions of different complexity. Section 3 illustrates and discusses experimental results. Conclusions and future work (Section 4) end the paper.

2 METHOD DESCRIPTION

Let us have a *dataset* defined as a set of N object-label pairs. Each object is described by a vector of *features* drawn from a feature space $\mathcal{X}$. The label associated with each object is an element of a finite set of *classes* $\mathcal{Y}$. We can then write $\mathcal{D} = \{(\mathbf{x_i}, y_i), i = 1, \ldots, N\}$. In the following, with a small abuse of notation, we will write $\mathbf{x} \in \mathcal{D}$ to refer to the feature vector of an element in the dataset, and $y(\mathbf{x})$ to refer to the observed label associated to it. As the method we are proposed has only been tested on binary datasets, for convenience we will assume that $\mathcal{Y} = \{-1, +1\}$.

A *classifier* for a dataset $\mathcal{D}$ is a computable function c which returns a *predicted* label for an object given as input. In general, the form of c is independent of the dataset, and a set of parameters need to be set. When the predicted label differs from the true one present in the dataset, we say that the classifier has committed an error.

A *training algorithm* for a classifier c over a *training dataset* $\mathcal{T}$ (often $\mathcal{T} \subset \mathcal{D}$) is an algorithm which takes the elements of $\mathcal{T}$ as examples to set the free parameters of c. Often, the parameters are set to minimize the number of errors over the training set, but various refinements may be used to try to reduce the number of errors on unseen instances.

What we propose is a method to identify the inherent complexity of groups of elements in the dataset, so that it can be split into regions of different complexity. We will show that the method is always capable of separating the "hard" regions (in which the classification accuracy is always less than 50%) from the "easy" and "average" regions.

MRCA operates according to the following steps:

1. Define a transformation able to map elements of the given dataset to a *profile space* $\mathcal{P}$ and apply the transformation to every element in the dataset;
2. Cluster the items in the profile space –with the underlying assumption that items with similar complexity occur close to each other in this space;
3. Evaluate the inherent complexity of each cluster and rank clusters according to a complexity metric called *multiresolution index* (*MRI* for short).

Our algorithm has to be applied on the "training" part of the dataset, as it needs to know the class label $y\mathbf{x}$ of each instance $\mathbf{x}$.

2.1 First Step: Generating a Profile Space

The first step is aimed at facilitating the task of estimating the complexity of a sample $\mathbf{x} \in \mathcal{D}$. To this end, we apply a technique called *multiresolution analysis*. We estimate the complexity of the sample by drawing around it hyper spheres of different radii. The content of each hypersphere is then analyzed by means of a lightweight but effective complexity metric, called *imbalance estimation function*. Given a set of examples $\mathcal{D}$, and recalling that $\mathcal{Y} = \{-1, +1\}$, the imbalance estimation function is defined as follows:

$$\psi_{\mathcal{D}}(\mathbf{x}, \sigma) = y(\mathbf{x}) \cdot \frac{\sum_{\mathbf{x}'_c \in \mathcal{D}} y(\mathbf{x}'_c) \cdot \phi_\sigma(\mathbf{x}, \mathbf{x}')}{\sum_{\mathbf{x}'_c \in \mathcal{D}} \phi_\sigma(\mathbf{x}, \mathbf{x}')} \quad \forall \mathbf{x} \in \mathcal{D} \tag{1}$$

where $\mathbf{x}$ is the center of the current hypersphere, whose extension is controlled by the *scale factor* σ, $\mathbf{x}'_c$ is a generic feature vector in $\mathcal{D}$, and $\phi_\sigma(\mathbf{x}, \mathbf{x}')$ is a function (*probe* hereinafter) devised to account for the importance of $\mathbf{x}'_c$ with respect to the object $\mathbf{x}$ under analysis. As a design choice, the probe is also entrusted with checking whether $\mathbf{x}'_c$ is within the current hypersphere or not. In particular, the value returned by the probe will be zero when $\mathbf{x}'_c$ is outside it. The simplest definition for the probe would be a sharp boundary checker, which returns 0 outside the hypersphere and 1 inside. A more sophisticated policy would constrain ϕ to play the role of a fuzzy membership function, entrusted with asserting to which extent the sample $\mathbf{x}'_c$ belongs to the probe centered in $\mathbf{x}$. In this case, a value in the range $[0, 1]$ would be returned when $\mathbf{x}'_c$ is inside the hypersphere, depending on its proximity with $\mathbf{x}$ (the closer the higher). It can be easily shown that, by definition, ψ ranges in $[-1, +1]$. In particular:

- $\psi \approx -1$ indicates a strong imbalance among the samples that occur within the probe, with labeling mostly different from the one of $\mathbf{x}$;
- $\psi \approx 0$ indicates that positive and negative samples are equally distributed within the probe;

- $\psi \approx +1$ indicates a strong imbalance among the samples that occur within the probe, with labeling mostly equal to the one of $\mathbf{x}$.

The number of hyper spheres being m, each sample $\mathbf{x} \in \mathcal{D}$ would be described in the profile space $\mathcal{P}$ by a vector of m components. A *profile* $\mathbf{p} \in \mathcal{P}$ for an $\mathbf{x} \in \mathcal{D}$ is obtained by repeatedly varying the scale factor in ψ, which forces the generation and evaluation of probes with different size. The set of adopted scale factors $\{\sigma_1, \sigma_2, \ldots, \sigma_m\}$ must be drawn in accordance with the wanted size of the profile, with the additional constraint that $\sigma_1 < \sigma_2 < \ldots < \sigma_m$. In doing so, the profile for a sample $\mathbf{x} \in \mathcal{D}$ is given by:

$$\mathbf{p} = [\psi_{\mathcal{D}}(\mathbf{x}, \sigma_1), \ldots, \psi_{\mathcal{D}}(\mathbf{x}, \sigma_m)] = \Psi_{\mathcal{D}}(\mathbf{x}) \quad (2)$$

Applying the profile transformation Ψ to every element in a set of instances $\mathcal{D}$ gives rise to a set of *profile patterns* $\mathcal{D}_P$, with elements belonging to the profile space $\mathcal{P} = [-1, +1]^m$.

We would like to stress that to apply the profile transformation, we need both the feature vector and the label associated with it.

2.2 Step Two: Clustering the Profile Space

Applying centroid-based clustering to $\mathcal{D}_P$ allows to identify regions characterized by different degrees of classification complexity. Assuming that a distance function d is defined in $\mathcal{P}$, each cluster can be identified by its proper centroid, yielding a set of r centroids:

$$\mathcal{C} = \{\, \mathbf{p}^{(k)} \,|\, k = 1, 2, \ldots, r \,\} \quad (3)$$

The k-th element of the underlying partition over $\mathcal{D}_P$ is defined as:

$$\mathcal{D}_P^{(k)} = \{\, \mathbf{p} \in \mathcal{D}_P \,|\, f_k(\mathbf{p}) = 1 \,\} \quad k = 1, \ldots, r \quad (4)$$

where $f_k : \mathbf{p} \to \{0, 1\}$ is the characteristic function for the k-th cluster, which relies on the distance function as follows:

$$f_k(\mathbf{p}) = \begin{cases} 1 & k = \underset{1 \le j \le r}{\arg\min}\, d(\mathbf{p}, \mathbf{p}^{(j)}) \\ 0 & \text{otherwise} \end{cases} \quad (5)$$

As for each $\mathbf{x} \in \mathcal{D}$ a correspondent $\mathbf{p} \in \mathcal{D}_P$ exists, also the original dataset $\mathcal{D}$ can be clustered accordingly. In symbols:

$$\mathcal{D}^{(k)} = \{\, (\mathbf{x}, y(\mathbf{x})) \,|\, \Psi(\mathbf{x}) \in \mathcal{D}_P^{(k)} \,\} \quad k = 1, \ldots, r \quad (6)$$

2.3 Step Three: Complexity Estimation

The third step of the proposed method is aimed at estimating the complexity of each cluster, with the goal of ranking them according to their complexity.

To estimate the complexity, we defined a simple metric called *Multi Resolution Index*. The *MRI* can be calculated for an element in $\mathcal{D}_P$ or for a cluster. In either case, it ranges in [0, 1] (the higher the value is, the more complex the corresponding pattern or cluster is). We decided to adopt a cumulative strategy, which uses the first kind of *MRI* to evaluate the second.

As for a single pattern $\mathbf{p} \in \mathcal{P}$, we realized that the components of a profile with finer granularity carry more information about the difficulty of classifying a pattern. To take into account this aspect, we opted to weight the components according to the size of the probe. In particular, the *MRI* of a pattern in the profile space is defined as:

$$MRI(\mathbf{p}) = \frac{1}{2m} \cdot \sum_{j=1}^{m} w_j \cdot [1 - p_j] \quad (7)$$

where w_j $(j = 1, 2, \ldots, m)$ denote weights applied to the components of $\mathbf{p}$. In particular, to implement a policy that weights more the components with finer granularity, one may get the actual values $[w_1, w_2, \ldots, w_m]$ as samples of a monotonically decreasing function.

To compute the *MRI* of a cluster, we average the adopted metric on the patterns that belong to the cluster:

$$MRI^{(k)} = \frac{1}{|\mathcal{D}_P^{(k)}|} \cdot \sum_{\mathbf{p} \in \mathcal{D}_P^{(k)}} MRI(\mathbf{p}) \quad (8)$$

$MRI^{(k)}$ is expected to yield small values when the k-th cluster is characterized by a strong imbalance that agrees with the labeling of the cluster elements themselves, as $\psi \approx 1$. The worst case occurs when the imbalance is against the labeling of the cluster elements, which yields $MRI^{(k)} \approx 1$. In case of a balanced cluster, $MRI^{(k)} \approx \frac{1}{2}$. As a final note on the proposed method, let us point out that, by virtue of the backward mapping between the clusters in $\mathcal{D}_P$ and the clusters in $\mathcal{D}$, the ranking holds also for $\mathcal{D}^{(k)}$ – notwithstanding the fact that the samples corresponding to the components of a cluster are typically scattered along the feature space rather than being close to each other.

3 EXPERIMENTAL RESULTS

3.1 Parameters Setting

The proposed method is customizable along several dimensions, which are preliminarily summarized below.

Shape of the probe. As already pointed out, we assume the probe be spherically shaped [1]. According to this assumption, a probe will be completely characterized by the reference sample $\mathbf{x}$ and by the radius σ of the hypersphere. The adopted probing function ϕ is the boundary checker, defined as:

$$\phi_\sigma(\mathbf{x},\mathbf{x}') = \begin{cases} 1 & \|\mathbf{x}'-\mathbf{x}\| \leq \sigma \\ 0 & \text{otherwise} \end{cases} \quad (9)$$

In agreement with Equation 9, the imbalance estimation function defined in Equation 1 can be rewritten as:

$$\psi_D(\mathbf{x},\sigma) = y(\mathbf{x}) \cdot \frac{N_\sigma^+(\mathbf{x}) - N_\sigma^-(\mathbf{x})}{N_\sigma^+(\mathbf{x}) + N_\sigma^-(\mathbf{x})} \quad (10)$$

where $N_\sigma^+(\mathbf{x})$ and $N_\sigma^-(\mathbf{x})$ are the number of patterns in D with label $+1$ and -1 in the hypersphere with center $\mathbf{x}$ and radius σ.

Distance measure. In the experiments we adopted the Euclidean distance, defined as:

$$d(\mathbf{p},\mathbf{p}') = \sqrt{\sum_{j=1}^{m} \left[\mathbf{p}_j - \mathbf{p}'_j\right]^2} \quad \mathbf{p},\mathbf{p}' \in \mathcal{P} \quad (11)$$

Of course, other distance metrics are also applicable (e.g., a la mode of p-norms).

Cardinality of the profile space. We ran the experiments with multiple values for the cardinality of the transformed space. Experiments have been run with a value for m that falls between 10 and 50.

Scaling strategy. The radius of the probe is scaled linearly using the scale factor σ up to the greatest value σ_{max}, which is calculated as the value of the radius for which the corresponding hypersphere contains (on average) a fixed percentage of the dataset elements, say ρ. We ran our experiments with $\rho = 0.05, 0.1, 0.15, 0.2$. The expression for σ_j is given by:

$$\sigma_j = \frac{j}{m} \cdot \sigma_{max} \quad j = 1,2,\ldots,m \quad (12)$$

Weighting policy. The weighting policy has been defined in accordance with the adopted scaling strategy. We imposed a linear behavior also to this function. In symbols:

$$w_j = 1 - \frac{j-1}{m} \quad j = 1,2,\ldots,m \quad (13)$$

Partitioning strategy and cardinality of the partition. The k-means algorithm has been adopted to implement the clustering strategy. The choice felt to k-means, due to its simplicity among the centroid-based clustering algorithms. It turns out that its main limitation, namely the need for specifying the number of clusters by hand, was in fact useful in this setting. Experiments have been run varying the number of clusters from 3 to 5. In particular, with $r = 3$, we were expecting the cluster algorithm to identify a "hard" cluster and an "easy" cluster, together with a medium complexity cluster.

[1] In presence of clear differences among the dimensions of the feature space, which can be put into evidence by calculating the covariance matrix from the available samples, one may decide to preliminarily equalize the space.

3.2 Datasets

To assess the validity of the proposed method, we performed experiments on various binary datasets. We opted for the KEEL repository (Alcalá-Fdez et al., 2011), which contains several binary datasets able to guarantee the statistical significance of experimental results. The selected datasets are characterized as follows:

Type of features. We have selected only datasets with only real-valued features.

Dimensionality of the feature space. With the goal of testing the effectiveness of the proposed method on different feature spaces, we selected datasets whose number of features goes from 2 to 57.

The selected datasets are summarized in Table 2. Some of them are also hosted by the UCI repository (Bache and Lichman, 2013).

3.3 Results

We applied PCA to each dataset, reducing the number of features to 5. Then we applied a Mahalanobis transformation on the PCA-reduced feature space, in order to obtain a uniform covariance matrix (that is, as a result of the two transformations the covariance matrix of the sample becomes a 5×5 identity matrix). On this reduced feature space, we have run our complexity estimation algorithm for every combination of the parameters shown in Table 1, for a total of 300 experiments (60 for each dataset).

In order to assess the effectiveness of the partitioning strategy, we checked whether a correlation exists between the *MRI* of each cluster and the local complexity directly estimated by means of a classifier. We ran a 10-fold cross validation on each dataset, using decision trees as learning algorithm (with standard Weka (Hall et al., 2009) settings for C4.5). As performance metrics, we evaluated accuracy, F-Score and Matthews' correlation coefficient for each cluster.

Figure 1 shows the relation between *MRI* and accuracy when data are split into 3, 4 and 5 clusters (*MRI* indexes have been normalized for the sake

Table 1: Parameters used in the experiments.

Parameter	Symbol	Values
Profile size	m	10, 20, 30, 40, 50
% of samples in maximum probe	ρ	0.05, 0.10, 0.15, 0.20
Number of clusters	r	3, 4, 5

Table 2: Summary of the KEEL datasets used for experiments.

Name	Features	Size
Banana	2	5,300
Phoneme	5	5,404
Ring	20	7,400
Spambase	57	4,597
Twonorm	20	7,400

of readability). Figures 2 and 3 show the same relation between *MRI* and, respectively, F-score and Matthews' correlation coefficient.

To accurately quantify the relation between *MRI* and the performance metrics, we also calculated Pearson's correlation coefficient for each experiment. Tables 3, 4, and 5 report the average correlation (and confidence interval) calculated over all datasets between the *MRI* and accuracy, F-score and Matthews' correlation coefficient.

Table 3: Correlation between *MRI* and *accuracy*.

m	r	0.05	0.10	0.15
	3	98.1 ± 1.1	98.1 ± 1.3	98.2 ± 1.3
10	**4**	97.9 ± 1.3	96.9 ± 1.9	96.3 ± 1.3
	5	97.8 ± 1.5	97.0 ± 1.8	96.5 ± 1.8
	3	98.2 ± 1.2	98.1 ± 1.3	98.3 ± 1.3
20	**4**	97.9 ± 1.3	97.2 ± 1.8	96.8 ± 1.8
	5	98.0 ± 1.1	97.1 ± 2.0	96.5 ± 1.9
	3	98.2 ± 1.1	98.1 ± 1.3	98.2 ± 1.3
30	**4**	98.0 ± 1.3	97.3 ± 1.8	96.8 ± 1.8
	5	98.1 ± 1.0	97.1 ± 1.8	96.8 ± 1.9
	3	98.3 ± 1.1	98.2 ± 1.3	98.3 ± 1.3
40	**4**	98.0 ± 1.2	97.2 ± 1.8	96.9 ± 1.8
	5	98.1 ± 1.0	97.2 ± 1.7	96.7 ± 1.9
	3	98.3 ± 1.1	98.2 ± 1.2	98.3 ± 1.3
50	**4**	98.0 ± 1.2	97.3 ± 1.8	96.9 ± 1.8
	5	98.0 ± 1.0	97.2 ± 1.7	96.7 ± 1.9

3.4 Discussion

As experimental results show, *MRI* is *always successful* at sorting clusters in decreasing order of classification accuracy, and its performance is stable over a broad range of different classification domains and configuration parameters (in particular, its performance is clearly independent of the profile size m).

Table 4: Correlation between *MRI* and *F-Score*.

m	r	0.05	0.10	0.15
	3	96.8 ± 2.2	96.2 ± 3.1	97.6 ± 1.3
	4	97.0 ± 1.6	95.5 ± 1.7	87.0 ± 14.4
10	**5**	91.7 ± 9.0	89.0 ± 12.3	87.3 ± 14.9
	3	97.0 ± 2.0	96.5 ± 2.6	97.7 ± 1.3
	4	97.1 ± 1.6	95.8 ± 1.8	95.0 ± 1.9
20	**5**	92.4 ± 8.0	89.7 ± 11.8	87.6 ± 14.8
	3	97.0 ± 2.0	96.5 ± 2.7	97.7 ± 1.3
	4	97.2 ± 1.6	96.0 ± 1.7	95.1 ± 1.9
30	**5**	92.6 ± 8.2	90.0 ± 11.4	87.9 ± 14.2
	3	97.1 ± 1.9	96.6 ± 2.5	97.7 ± 1.3
	4	97.2 ± 1.6	96.0 ± 1.8	95.2 ± 1.8
40	**5**	92.6 ± 8.1	90.0 ± 11.5	88.0 ± 14.1
	3	97.1 ± 1.9	96.6 ± 2.5	97.7 ± 1.3
	4	97.2 ± 1.6	96.0 ± 1.7	95.2 ± 1.9
50	**5**	92.7 ± 7.7	90.0 ± 11.8	88.1 ± 14.1

Table 5: Correlation between *MRI* and *Matthews' correlation coefficient*.

m	r	0.05	0.10	0.15
	3	97.5 ± 0.6	97.1 ± 0.9	97.0 ± 1.2
	4	96.0 ± 2.7	94.9 ± 2.5	93.4 ± 4.4
10	**5**	94.6 ± 5.3	92.8 ± 7.1	92.5 ± 6.8
	3	97.6 ± 0.6	97.3 ± 0.8	97.2 ± 1.1
	4	96.1 ± 2.7	95.2 ± 2.5	94.7 ± 2.6
20	**5**	95.1 ± 4.6	93.5 ± 5.9	92.6 ± 6.5
	3	97.6 ± 0.6	97.3 ± 0.9	97.2 ± 1.2
	4	96.2 ± 2.8	95.1 ± 2.8	94.7 ± 2.6
30	**5**	95.0 ± 4.9	93.3 ± 6.2	92.9 ± 6.6
	3	97.6 ± 0.6	97.3 ± 0.8	97.3 ± 1.0
	4	96.2 ± 2.7	95.2 ± 2.6	94.7 ± 2.6
40	**5**	95.1 ± 4.7	93.7 ± 5.7	93.0 ± 6.2
	3	97.6 ± 0.6	97.3 ± 0.8	97.3 ± 1.1
	4	96.1 ± 3.0	95.2 ± 2.7	94.7 ± 2.7
50	**5**	95.0 ± 4.8	92.9 ± 7.1	93.1 ± 6.2

The best performance is obtained with three clus-

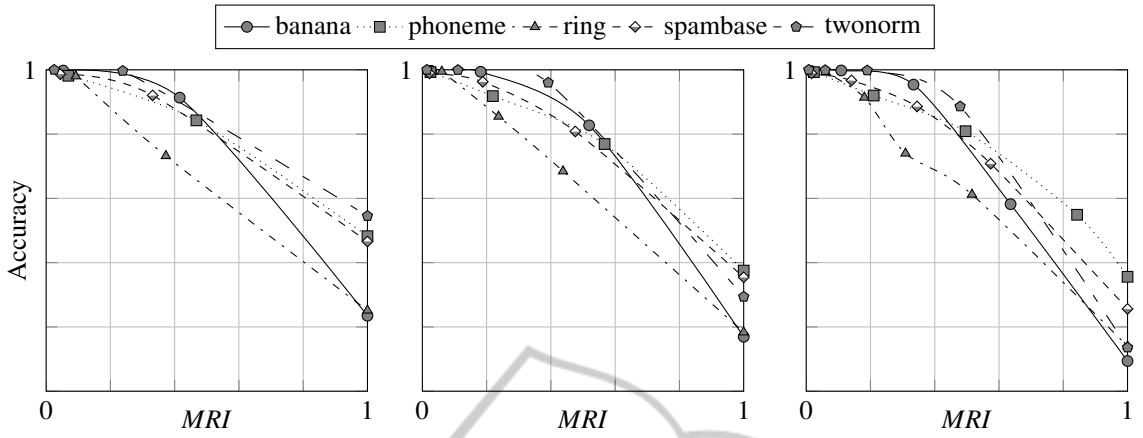

(a) $r = 3$ (b) $r = 4$ (c) $r = 5$

Figure 1: *MRI* v. accuracy, with $m = 30$, $\rho = 0.1$.

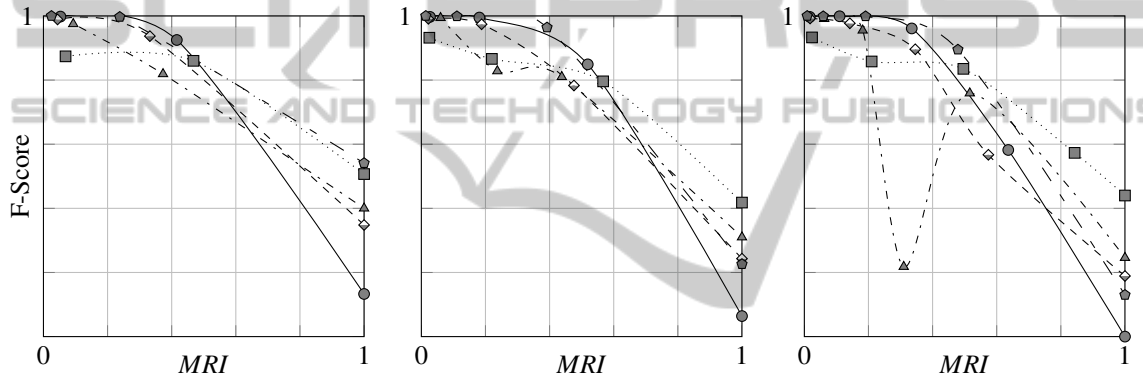

(a) $r = 3$ (b) $r = 4$ (c) $r = 5$

Figure 2: *MRI* v. F-Score, with $m = 30$, $\rho = 0.1$.

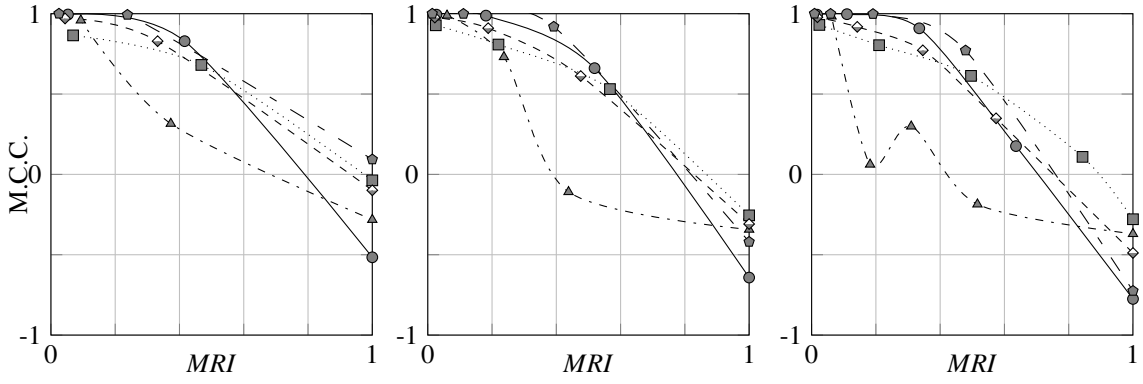

(a) $r = 3$ (b) $r = 4$ (c) $r = 5$

Figure 3: *MRI* v, Matthews' correlation, with $m = 30$, $\rho = 0.1$.

ters, which allow to split the dataset into hard, easy, and medium complexity clusters. In particular, as Figures 1a, 2a and 3a clearly highlight, the proposed method has demonstrated very useful to identify hard regions of the datasets in hand. In particular, the performance metrics are 50% or less for "hard" clusters.

When the number of clusters increase, the correlation between *MRI* and F-Score and Matthews' cor-

relation coefficient tends to be lower than the correlation between *MRI* and accuracy. Figures 2 and 3 show that there is actually only one outlier dataset, namely the Ring dataset, for which we provide further discussion.

The choice of ρ, the average percent of samples embodied by the probe with greatest size, slightly influences the performance of the *MRI*. The reported tables show that the optimal choice is $\rho = 0.05$. Greater values of ρ decrease the performance of the *MRI* for ranking purposes. However, this phenomenon is largely expected, as increasing values of ρ force the algorithm to concentrate on greater hyper spheres, gradually shadowing its ability of performing a local analysis.

4 CONCLUSIONS

In this work, a method for partitioning datasets into regions of different classification complexity has been proposed. The method relies on a specific metric, called *MRI*, which is typically used for clustering the elements of a dataset into three regions of increasing classification complexity, thus separating the "easy" part of the data from the "hard" part (possibly due to noise). Increasing the number of clusters up to five does not decrease the ranking capacity of the *MRI*, except for particular datasets and only when compared with F-Score or Matthews' correlation coefficient. Moreover, the proposed method proved to be stable and effective for the majority of experiments and parameter settings.

Further work on the *MRI* will be carried out along both theoretical and experimental directions. Studies on statistical significance of *MRI* estimates may help to discover a lower bound on the optimal number of clusters to be used for splitting a dataset. We are also planning to substitute the imbalance estimation function with a local correlation estimation, aimed at separating linearly separable areas (which are typically easy to classify), from noisy areas, as these two would have the same imbalance but different local correlation indexes.

ACKNOWLEDGEMENTS

Emanuele Tamponi gratefully acknowledges Sardinia Regional Government for the financial support of his PhD scholarship (P.O.R. Sardegna F.S.E. Operational Programme of the Autonomous Region of Sardinia, European Social Fund 2007-2013 - Axis IV Human Resources, Objective l.3, Line of Activity l.3.1.).

REFERENCES

Abdi, H. and Williams, L. J. (2010). Principal component analysis. *Wiley Interdisciplinary Reviews: Computational Statistics*, 2:433—-459.

Alcalá-Fdez, J., Fernández, A., Luengo, J., Derrac, J., and García, S. (2011). Keel data-mining software tool: Data set repository, integration of algorithms and experimental analysis framework. *Multiple-Valued Logic and Soft Computing*, 17(2-3):255–287.

Bache, K. and Lichman, M. (2013). UCI machine learning repository.

Bhattacharyya, A. (1943). On a measure of divergence between two statistical populations defined by their probability distributions. *Bulletin of Cal. Math. Soc.*, 35(1):99–109.

Fukunaga, K. (1990). *Introduction to statistical pattern recognition (2nd ed.)*. Academic Press Professional, Inc., San Diego, CA, USA.

Hall, M., Frank, E., Holmes, G., Pfahringer, B., Reutemann, P., and Witten, I. H. (2009). The weka data mining software: an update. *SIGKDD Explor. Newsl.*, 11(1):10–18.

Ho, T. (2000). Complexity of classification problems and comparative advantages of combined classifiers. In *Multiple Classifier Systems*, volume 1857 of *Lecture Notes in Computer Science*, pages 97–106. Springer Berlin Heidelberg.

Ho, T. K. and Basu, M. (2000). Measuring the complexity of classification problems. In *in 15th International Conference on Pattern Recognition*, pages 43–47.

Luengo, J., Fernández, A., García, S., and Herrera, F. (2011). Addressing data complexity for imbalanced data sets: analysis of smote-based oversampling and evolutionary undersampling. *Soft Computing*, 15(10):1909–1936.

Luengo, J. and Herrera, F. (2012). Shared domains of competence of approximate learning models using measures of separability of classes. *Information Sciences*, 185(1):43 – 65.

Mahalanobis, P. C. (1930). On tests and measures of group divergence. Part 1. Theoretical formulae. *Journal and Proceedings of the Asiatic Society of Bengal (N.S.)*, 26:541–588.

Mansilla, E. B. and Ho, T. K. (2005). Domain of Competence of XCS Classifier System in Complexity Measurement Space.

Pierson, W. E., Jr., and Pierson, W. E. (1998). Using boundary methods for estimating class separability.

Pierson, W. E., Ulug, B., Ahalt, S. C., Sancho, J. L., and Figueiras-Vidal, A. (1998). Theoretical and complexity issues for feature set evaluation using boundary methods. In Zelnio, E. G., editor, *Algorithms for Synthetic Aperture Radar Imagery V*, volume 3370 of *Society of Photo-Optical Instrumentation Engineers (SPIE) Conference Series*, pages 625–636.

Singh, S. (2003). Multiresolution estimates of classification complexity. *Pattern Analysis and Machine Intelligence, IEEE Transactions on*, 25(12):1534–1539.

Sohn, S. Y. (1999). Meta analysis of classification algorithms for pattern recognition. *IEEE Trans. Pattern Anal. Mach. Intell.*, 21(11):1137–1144.

Sotoca, J. M., Mollineda, R. A., and Sánchez, J. S. (2006). A meta-learning framework for pattern classification by means of data complexity measures. *Inteligencia Artificial, Revista Iberoamericana de Inteligencia Artificial*, 10(29):31–38.

Tumer, K. and Ghosh, J. (1996). Estimating the bayes error rate through classifier combining. In *In Proceedings of the International Conference on Pattern Recognition*, pages 695–699.